IC/86/22

INTERNATIONAL CENTRE FOR
THEORETICAL PHYSICS

RESTRICTED PRIMITIVE MODEL FOR ELECTRICAL DOUBLE LAYERS:
MODIFIED HNC THEORY OF DENSITY PROFILES
AND MONTE CARLO STUDY OF DIFFERENTIAL CAPACITANCE

P. Ballone

G. Pastore

and

M.P. Tosi

**INTERNATIONAL
ATOMIC ENERGY
AGENCY**

**UNITED NATIONS
EDUCATIONAL,
SCIENTIFIC
AND CULTURAL
ORGANIZATION**

1986 MIRAMARE-TRIESTE

International Atomic Energy Agency

and

United Nations Educational Scientific and Cultural Organization

INTERNATIONAL CENTRE FOR THEORETICAL PHYSICS

RESTRICTED PRIMITIVE MODEL FOR ELECTRICAL DOUBLE LAYERS:
MODIFIED HNC THEORY OF DENSITY PROFILES
AND MONTE CARLO STUDY OF DIFFERENTIAL CAPACITANCE *
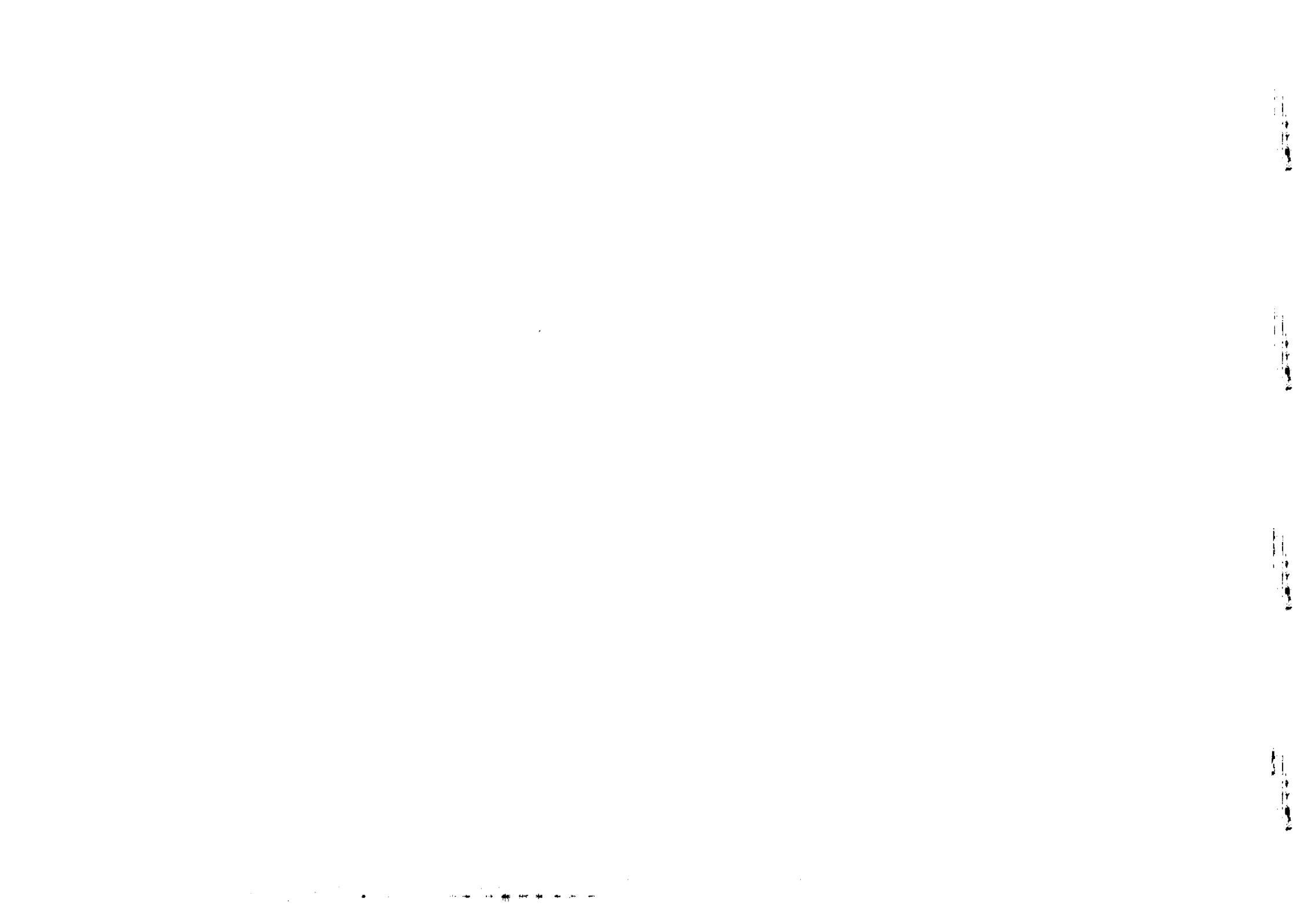
P. Ballone and G. Pastore
International School for Advanced Studies, Trieste, Italy

and

M.P. Tosi
International Centre for Theoretical Physics, Trieste, Italy
and
Dipartimento di Fisica Teorica dell'Università di Trieste, Trieste, Italy.

MIRAMARE – TRIESTE

February 1986

* To be submitted for publication.

ABSTRACT

Interfacial properties of an ionic fluid next to a uniformly charged
planar wall are studied in the restricted primitive model by both theoretical
and Monte Carlo methods. The system is a 1:1 fluid of equisized charged
hard spheres in a state appropriate to 1M aqueous electrolyte solutions.
The interfacial density profiles of counterions and coions are evaluated by
extending the hypernetted chain approximation (HNC) to include the leading
bridge diagrams for the wall-ion correlations. The theoretical results compare
well with those of grand canonical Monte Carlo computations of Torrie and
Valleau over the whole range of surface charge density considered by these
authors, thus resolving the earlier disagreement between statistical mechanical
theories and simulation data at large charge densities. In view of the
importance of the model as a testing ground for theories of the diffuse layer,
the Monte Carlo calculations are tested by considering alternative choices for
the basic simulation cell and are extended so as to allow an evaluation of the
differential capacitance of the model interface by two independent methods.
These involve numerical differentiation of the mean potential drop as a function
of the surface charge density or alternatively an appropriate use of a
fluctuation theory formula for the capacitance. The results of these two
Monte Carlo approaches consistently indicate an initially smooth increase of
the diffuse layer capacitance followed by structure at large charge densities,
this behaviour being connected with layering of counterions as already
revealed in the density profiles reported by Torrie and Valleau.

1.   INTRODUCTION

For a long time there has been considerable interest, both fundamental
and applied, in the theory of the electrical double layer formed by charge
separation at the interface between two polarizable media. A well known example
is the interface between a blocking metallic electrode and an electrolyte
solution [1]. The complexity of the physical situation at such an interface has
motivated the study of models which, though crude, shed light on important
aspects of the problem. In particular the restricted primitive model, which
considers a binary fluid of equisized charged hard spheres facing a charged
hard wall in a uniform dielectric medium, is believed to reflect the basic
statistical-mechanical behaviour of the ionic component of an electrolyte
solution in the electric field created by a planar distribution of external
charge.

A great number of approximate theories, having their counterpart in
theories of bulk liquid structure, have been examined for the restricted
primitive model of the metal/electrolyte interface [2],[3]. A decisive step
forward was taken by Torrie and Valleau [4], who brought Monte Carlo methods
in computer simulation to bear on the understanding of the model. They
studied it in a state appropriate to 1:1 aqueous electrolyte solutions, with
special attention to concentrations of 0.01 M, 0.1 M and 1.0 M over a wide
range of values for the surface charge density. They used their data for
quantitative tests of various approximate theories of the potential drop and
the ionic density profiles in the diffuse layer (see also the review of Carnie
and Torrie [3]). A remarkable behaviour was found in the model at high
concentrations and surface charge densities, i.e. a layering of counterions
next to the wall which leads to a large value of the potential drop. This
behaviour was not shown by any of the available theories. Some of these
actually predict a negative contribution of the diffuse layer to the inverse
capacitance of the interface at moderately large values of the surface charge
density, which is in qualitative conflict with the data.

We develop further in this paper the study of the model by both
theoretical and Monte Carlo simulation methods, with specific attention to
the high concentration state already studied by Torrie and Valleau.
Theoretically, we examine the next step in the development of cluster expansions
for the fluid at the interface, leading to modification of the hypernetted
chain approximation (HNC) by the inclusion of the leading bridge diagrams for
the correlations between the charged wall and the ions in the electrolyte.

We find that essential agreement with the Monte Carlo data is achieved at this stage of the theory. We also extend the Monte Carlo study of the model to test some aspects of the simulation set-up and to obtain an estimate of its electrical capacitance curve.

The ionic fluid in our computations is made of charged spheres with charge $\pm e$ and diameter d at concentration 1 M and temperature T, next to a hard wall which carries a uniform surface charge density σ. The whole system is immersed in a uniform medium with dielectric constant ε, i.e. image charge effects between the fluid and the wall are absent. We take for the reduced temperature $\beta^* = e^2/(\varepsilon k_B T d)$ the value $\beta^* = 1.6809$, which corresponds to $\varepsilon = 78.5$, $T = 298$ K and $d = 4.25$ Å. Sec. 2 presents the modified HNC theory of this model and its results. The Monte Carlo computations and some of their results are presented in Sec. 3, while Sec. 4 discusses specifically the evaluation of the diffuse layer capacitance. A brief discussion and summary are given in Sec. 5.

2. MODIFIED HNC THEORY OF THE INTERFACE

As is well known, the free energy of an inhomogeneous multicomponent system in a set of external potentials $\varphi_\alpha(\underline{r})$ acting on α-type particles is a functional of the particle density profiles $n_\alpha(\underline{r})$. At equilibrium with a homogeneous bulk state having particle densities n_α, the equilibrium conditions for the density profiles can be written by means of a formally exact functional expansion [5] in the form

$$\ln\left\{ \frac{n_\alpha(\underline{r})}{n_\alpha} \exp\left[\varphi_\alpha(\underline{r})/k_B T\right]\right\} = \sum_\beta n_\beta \int d\underline{r}' \, c^{(2)}_{\alpha\beta}(|\underline{r}-\underline{r}'|) h_\beta(\underline{r}')$$
$$+ \frac{1}{2}\sum_{\beta,\gamma} n_\beta n_\gamma \iint d\underline{r}' d\underline{r}'' \, c^{(3)}_{\alpha\beta\gamma}(\underline{r},\underline{r}',\underline{r}'') h_\beta(\underline{r}') h_\gamma(\underline{r}'') + \cdots \quad . \quad (2.1)$$

In Eq.(2.1) we have defined

$$h_\alpha(\underline{r}) = [n_\alpha(\underline{r}) - n_\alpha]/n_\alpha \qquad (2.2)$$

and the c's are the bulk 2-body and 3-body direct correlation functions. Truncation of the right-hand side of Eq.(2.1) at the 2-body term yields the HNC, while the 3-body and higher order terms are the counterpart of the bridge diagram contributions in the theory of correlations in homogeneous fluids.

Considerable experience has been gained in recent years on the estimation of bridge functions in the calculation of bulk liquid structure. In particular Bacquet and Rossky [6] working on electrolyte solutions and Iyetomi and Ichimaru [7] working on the classical one-component plasma have shown that a useful approximation consists in including the 3-body term through an assumption of superposition for the 3-body direct correlation function in terms of the bulk total correlation functions $h_{\alpha\beta}(r)$, i.e.

$$c^{(3)}_{\alpha\beta\gamma}(\underline{r},\underline{r}',\underline{r}'') = h_{\alpha\beta}(|\underline{r}-\underline{r}'|) h_{\beta\gamma}(|\underline{r}'-\underline{r}''|) h_{\gamma\alpha}(|\underline{r}''-\underline{r}|) \quad . \quad (2.3)$$

In their discussion of electrolyte structure Bacquet and Rossky [6] point out that their inclusion of leading bridge diagrams by the above approximation successfully corrects for an underestimate of the correlation hole between like ions in the HNC and for its consequences on the distribution of unlike ions around a given ion. Qualitatively similar defects can be seen in the HNC density profiles of coions and counterions next to a charged wall at large values of the surface charge density.

2.1 Explicit equations for planar interface

In our approach to the local structure of an electrolyte next to a charged hard wall, we include the bridge corrections to the HNC for the wall-ion correlations (i.e. for the density profiles) by the approximation given in Eq.(2.3). Fig. 1 shows that we are thereby including in the wall-ion correlations the effect of correlations of the ion with pairs of ions which are correlated with the wall and with each other. All the ion-ion correlations are described by bulk total correlation functions $h_{\alpha\beta}(r)$, that we evaluate in the HNC.

Setting the edge of the wall at $z = -\frac{1}{2} d$ and specializing Eqs.(2.1) to (2.3) to the geometry of the present problem, the equilibrium condition for the density $n_\alpha(z) \equiv n_\alpha[1 + h_\alpha(z)]$ of ions with valence Z_α at position z takes the form

$$\begin{cases} \ln[1 + h_\alpha(z)] = -\dfrac{Z_\alpha e}{k_B T}\psi(z) + \Phi_\alpha(z) + E^{(4)}_\alpha(z) & (z > 0) \\[2ex] h_\alpha(z) = -1 & (z < 0) \end{cases} \qquad (2.4)$$

-3-

-4-

Here, $\psi(z)$ is the electrostatic potential, $\Phi_\alpha(z)$ gives the HNC term and $E_\alpha^{(4)}(z)$ is the bridge term in our approximation. Explicitly $\Phi_\alpha(z)$ is given by [8),9)]

$$\Phi_\alpha(z) = 2\pi \sum_\beta n_\beta \int_{-\infty}^{\infty} dz'\, h_\beta(z') \int_{|z-z'|}^{\infty} ds\, s\, c_{\alpha\beta}^{SR}(s) \qquad (2.5)$$

where

$$c_{\alpha\beta}^{SR}(r) = c_{\alpha\beta}^{(2)}(r) + Z_\alpha Z_\beta e^2/(\varepsilon r k_B T). \qquad (2.6)$$

With reference to Fig. 1, where the two intervening ions are at positions $\underline{r}_1 = (R_1, z_1, 0)$ and $\underline{r}_2 = (R_2, z_2, \varphi)$ in cylindrical coordinates, the expression of $E_\alpha^{(4)}(z)$ is

$$E_\alpha^{(4)}(z) = \tfrac{1}{2} \sum_{\beta,\gamma} n_\beta n_\gamma \int_{-\infty}^{\infty} dz_1\, h_\beta(z_1) \int_{-\infty}^{\infty} dz_2\, h_\gamma(z_2) \int_0^\infty R_1 dR_1 \int_0^\infty R_2 dR_2 \int_0^{2\pi} d\varphi\, h_{\alpha\beta}(r_{10}) h_{\alpha\gamma}(r_{20}) h_{\beta\gamma}(r_{12}) \qquad (2.7)$$

with

$$\left\{ \begin{array}{l} r_{10} = \left[R_1^2 + (z_1-z)^2 \right]^{1/2} \\[2mm] r_{20} = \left[R_2^2 + (z_2-z)^2 \right]^{1/2} \\[2mm] r_{12} = \left[(R_1 - R_2 \cos\varphi)^2 + R_2^2 \sin^2\varphi + (z_1-z_2)^2 \right]^{1/2}. \end{array} \right. \qquad (2.8)$$

The Eqs.(2.4) for the density profiles must be solved in conjunction with the Poisson equation for the electrostatic potential $\psi(z)$,

$$\frac{d^2\psi(z)}{dz^2} = -\frac{4\pi e}{\varepsilon} \sum_\alpha Z_\alpha n_\alpha h_\alpha(z) \qquad (z > 0) \quad, \qquad (2.9)$$

subject to the boundary conditions

$$\psi'(0) = -4\pi\sigma/\varepsilon \qquad (2.10)$$

and

$$\lim_{z \to \infty} \psi(z) = 0. \qquad (2.11)$$

-5-

2.2 Numerical method of solution

Badiali et al. [10)] have developed a very efficient numerical method for calculations on the interface between a hard wall and a classical one-component plasma, which preserves the boundary conditions on $\psi(z)$ at each iteration step even though the charge density profile may be going through non-neutral states. In an immediate extension of their method to the present problem, we simply add to the Poisson equation (2.9) a linear combination of the equilibrium equations (2.4) for the two ionic species, with coefficients chosen so as to optimize the stability of the boundary condition (2.11). The equation for $\psi(z)$ becomes

$$\frac{d^2\psi(z)}{dz^2} - k_D^2\,\psi(z) = -(4\pi e/\varepsilon) \sum_\alpha n_\alpha Z_\alpha \left\{ h_\alpha(z) - \ln\left[1 + h_\alpha(z)\right] + \Phi_\alpha(z) + E_\alpha^{(4)}(z) \right\} \qquad (2.12)$$

where

$$k_D = \left(4\pi e^2 \sum_\alpha n_\alpha Z_\alpha^2 / \varepsilon k_B T \right)^{1/2}. \qquad (2.13)$$

This ensures that fluctuations in $h_\alpha(z)$ occurring during the iterative process of solution at large distance from the wall lead only to second-order charges in the righ-hand-side of Eq.(2.12).

Eq.(2.12) with the boundary conditions (2.10) and (2.11) can be integrated to give

$$(\varepsilon k_D/2\pi e)\,\psi(z) = -\exp(k_D z) \int_z^\infty dz'\, T(z') \exp(-k_D z')$$
$$+ \exp(-k_D z)\left[\frac{2\sigma}{e} - \int_0^\infty dz'\, T(z') \exp(-k_D z') - \int_0^z dz'\, T(z') \exp(k_D z') \right] \qquad (2.14)$$

where

$$T(z) = \sum_\alpha n_\alpha Z_\alpha \left\{ \ln\left[1 + h_\alpha(z)\right] - h_\alpha(z) - \Phi_\alpha(z) - E_\alpha^{(4)}(z) \right\}. \qquad (2.15)$$

In our calculations we solve iteratively Eqs.(2.4) and (2.14) for given value of the bridge functions $E_\alpha^{(4)}(z)$, as specified immediately below. This approach, combined with optimized methods of mixing successive iterations as developed by Ng [11)], is very efficient and simple to implement numerically.

-6-

The calculations start with the solution of Eqs.(2.4) and (2.14) in the HNC, i.e. with $E_\alpha^{(4)}(z) = 0$. The HNC density profiles are used in Eq.(2.7) to obtain a first estimate of $E_\alpha^{(4)}(z)$ and hence modified profiles are obtained by renewed solution of Eqs. (2.4) and (2.14). The numerical results that we report below refer to this level of approximation. Although a fully consistent evaluation of the profiles and of the bridge functions would in principle be necessary, the computation of the integrals (2.7), which is carried out with a Monte Carlo numerical integrator, is very time consuming. Both the work of Bacquet and Rossby [6] on electrolyte solutions and our own work on molten salts [12] indicate that the first estimate of $E_\alpha^{(4)}(z)$ should already be reasonably close to full convergence. We estimate an uncertainty of the order of 5% in our results for the leading wall-ion bridge functions.

2.3   Numerical results

The interfacial structure has been evaluated by the above approach for three values of the reduced surface charge density $\sigma^* = \sigma d^2/e$, i.e. $\sigma^* = 0.25$, 0.42 and 0.70. The density profiles of counterions and coions in the HNC and in the modified HNC are compared with each other and with Monte Carlo data in Figs. 2 to 4. The Monte Carlo results shown in these figures have been obtained in this work by procedures that will be presented in detail in Sec. 3 below. It suffices at this stage to remark that they are in very good agreement with the original data of Torrie and Valleau [4].

Fig. 2 shows that the cluster expansion as approximated by the HNC is still quite close to convergence at a surface charge density which is already quite large ($\sigma^* = 0.25$ corresponds to $\sigma = 0.22C/m^2$ with our model parameters). At still larger values of σ^*, however, Figs. 3 and 4 show that the layering of counterions in the interfacial region and the accompanying expulsion of coions are the main new qualitative features of the Monte Carlo results which are completely missed in the HNC but approximately accounted for in our estimate of the wall-ion bridge functions. The form of these functions is shown in Fig. 5 for $\sigma^* = 0.42$. Although the structure that we find in the bridge functions is somewhat unexpected, the net effect relative to the HNC is equivalent to additional soft repulsions between the wall and the two ionic species, thus leading to the changes in the two density profiles which are seen in Fig. 3. Fully quantitative agreement with the Monte Carlo profiles is not yet achieved in our theoretical approach, as is also shown by Fig. 4.

Fig. 6 reports from various Monte Carlo simulation runs and from our theoretical calculations, the values of the reduced potential drop ψ^* across the diffuse layer as a function of σ^*, this being defined as $\psi^* = e\psi(0)/k_B T$. We only need to remark here that the modified HNC results for ψ^* are in very good agreement with the Monte Carlo data over the whole range of surface charge density. The failure of the HNC in the evaluation of ψ^* at large values of σ^* is already well known [3],[4] and is illustrated again in Fig. 6.

The deficiencies of the HNC theory in the present context have been attributed by Nielaba and Forstmann [13] to its use of bulk ion-ion correlation functions in the region near the wall, where the pile-up of counterions and the expulsion of coions create conditions which are very far from those in the bulk. They accordingly proposed a somewhat ad hoc modification of $c_{\alpha\beta}^{(2)}(r)$ in the interfacial region. It seems pleasing that a qualitatively correct interfacial structure emerges in our calculations from a systematic development of the basic theory. Of course, the bridge diagrams shown in Fig. 1 may also be reinterpreted as reflecting local changes in $c_{\alpha\beta}^{(2)}(r)$ determined by the local ionic density profiles.

2.4   Contact theorem

In concluding this section, we should comment on the quality of our results in relation to the so-called contact theorem [14], i.e. the condition of macroscopic equilibrium which relates the contact values $n_\alpha(0)$ of the ionic densities to the bulk pressure p and to the surface charge density σ,

$$k_B T \sum_\alpha n_\alpha(o) = p + 2\pi\sigma^2/\varepsilon . \tag{2.17}$$

The HNC is known to violate this exact relation by bringing in the isothermal bulk modulus in place of the pressure, but in the electrolytic regime this error is quite small and rapidly decreasing in importance as σ increases [3].

From our calculation of wall-ion bridge functions we find violations of Eq.(2.17) which are somewhat larger than in the HNC at the three charge densities that we have considered. For instance, our percentual error in $\sum_\alpha n_\alpha(0)$ is 0.5% at $\sigma^* = 0.70$. This defect may be intrinsic to our treatment of bridge diagrams at very short distance from the wall or merely due to inaccuracies in our numerical evaluation of Eq.(2.7).

3. MONTE CARLO SIMULATION

In the grand canonical Monte Carlo method developed by Torrie and Valleau [4] for studying the diffuse layer, one considers a basic simulation cell of ionic fluid which is part of an infinite slab confined between two parallel walls. The rest of the slab consists of replicas of the central cell having a charge distribution which is the average charge distribution of the central cell as measured over all preceding configurations. Sampling of configuration space is carried out at constant chemical potential corresponding to a given bulk density and temperature, thus allowing an unambiguous identification of the bulk fluid state that would be in equilibrium with the charged interface, notwithstanding the finite size of the sample. The data reported by Torrie and Valleau refer to a distribution of surface charge in which one wall is uniformly charged and the other is uncharged.

Our main aim is to extend the study of the model to give an assessment of its differential capacitance as a function of surface charge density. We need for this purpose high statistical accuracy in the potential drop across the double layer, while still paying attention to the role of the replicas and to interference between the two walls. As will be discussed in detail below, we have still basically followed the simulation method of Torrie and Valleau but we have carried out some tests on the dimensions of the central cell and comparatively examined the results of assuming different distributions of surface charge density on the two walls. We should remark already at this point that all our results agree with those of Torrie and Valleau whithin their respective statistical accuracies whenever comparison is possible, except perhaps at the highest value of the surface charge density. This can be seen from Fig. 6 for the potential drop in the diffuse layer, in which we show with different symbols the original data of Torrie and Valleau and the results that we have obtained by taking either the same distribution of surface charge as they did (one wall is charged and the other uncharged) or a configuration in which the two walls carry equal and opposite charge densities. We shall focus the detailed discussion below on the latter configuration.

In our simulation runs the two walls are placed at a distance $L = 15.0000$ d and the lateral width of the cell is $W = 11.6588$ d in both directions. The value of L is appreciably larger than those adopted by Torrie and Valleau at 1 M, while the value of W corresponds to that of their largest sample. The cell contains equal numbers of cations and anions, since the two wall charges balance each other. The interaction with the replicas is treated by their method and the grand canonical sampling is carried out by adding and subtracting a pair of ions every ten moves with a probability weighted by the chemical potential μ

of the bulk fluid as determined by Valleau and Cohen [15]. The potential drop is determined from a run of 10^6 moves and its statistical accuracy is assessed to be of the order of 5% by calculating its variance from the values obtained in twenty subruns of 5×10^4 moves. The effects of cell finiteness have been tested at $\sigma^* = 0.70$ by doubling the cell volume in two alternative ways, i.e. by increasing W by a factor $2^{1/2}$ in order to test the role of the replicas or by increasing L by a factor 2 in order to test the interference between the two walls. In both these tests the potential drop was found to vary only within statistical accuracy.

Taking the walls at equal and opposite charge densities presents some specific advantages for our purpose, but also some disadvantages. The main advantage is an increase in statistical accuracy, since (a) the amplitude of fluctuations is reduced by a stronger coupling between the walls and the fluid, and (b) two double layers are simultaneous being studied. Furthermore, the internal energy of the sample is more easily evaluated since the zero of the electrostatic potential is unambiguously fixed. Somewhat different fluctuations are evidently being explored during the grand canonical sampling, relative to a configuration in which only one of the confining walls is charged. The main disadvantage is a possible interference between the two double layers. We have tested this point, as already noted, both by doubling L at $\sigma^* = 0.70$ and by repeating the simulation in the configuration of Torrie and Valleau at various values of σ^* (see Fig. 6). We have also monitored the average fluid density in a slab of width 4 d at the centre of our cell, finding that it agrees with the known bulk density within a statistical accuracy of the order of a percent.

In summary, the $(\sigma, -\sigma)$ configuration yields results in essential agreement with those of the $(\sigma, 0)$ configuration and allows higher statistical accuracy with a smaller number of moves, provided that the separation between the two walls is at least as large as in our runs. Further tests and refinements could examine the (σ, σ) configuration and adopt suitably biased Monte Carlo methods (see e.g. Valleau and Whittington [16]).

The density profiles and the potential drop that we have obtained from the simulation runs have already been shown in Figs. 2 to 4 and in Fig. 6. Before proceeding to a discussion of the differential capacitance data in the next section, we report some additional results in Fig. 7. This shows the adsorption coefficients Γ_α for the two ionic species, defined as

$$\Gamma_\alpha = \int_0^{\frac{1}{2}(L-d)} dx \left[n_\alpha(x) - n_\alpha \right] \quad , \tag{3.1}$$

and the excess surface energy γ_e per unit area of charged wall, as evaluated from the excess energy of our simulation sample by subtraction of the bulk excess energy determined by Valleau and Cohen [15]. The statistical accuracy of the data in Fig. 7 is of order 5% at $\sigma^* \simeq 0.1$ and of order 1% at $\sigma^* \simeq 0.7$.

We notice from Fig. 7 that the adsorption coefficients vary smoothly with surface charge density, in spite of the layering of counterions which is shown by the detailed density profiles in Figs. 3 and 4. Snapshots of the distribution of ions as seen from the wall show that layering has already started at $\sigma^* = 0.3$, even though the first layer of counterions facing the wall is still far from being closely packed.

4. DIFFERENTIAL CAPACITANCE OF THE DIFFUSE LAYER

The inverse differential capacitance C_d^{-1} of the diffuse layer as a function of the surface charge density can be obtained by numerical differentiation of the results for the potential drop shown in Fig. 6. One has to bear in mind that numerical differentiation of data affected by noise is subject to serious uncertainties and may lead to spurious structures. We have therefore examined also an alternative route for the evaluation of C_d from the Monte Carlo runs. The potential drop across the cell in the $(\sigma, -\sigma)$ configuration is given by

$$\Delta\psi = (4\pi e/\varepsilon d)\left[<D> - L\sigma^*/d\right] \tag{4.1}$$

where $<D>$ is the average dipole moment of the fluid per unit area in reduced units. The capacitance is thus related to $\partial<D>/\partial\sigma^*$. We derive here a fluctuation-theory formula for this quantity, which is specifically applicable to our simulation sample in the $(\sigma, -\sigma)$ configuration.

The Hamiltonian of the sample containing N cations and N anions is

$$H_N(\sigma^*) = -\frac{4\pi e^2}{\varepsilon d}D\sigma^* + \sum_{i=1}^{2N}\varphi_i(z_i) + U_{pair} \tag{4.2}$$

where the various terms give the interaction of the ions with the surface charges, their interaction with the replicas as described by external potentials $\varphi_i(z_i)$, and the pair interactions between the ions in the cell. The grand canonical partition function, subject to the restriction of equal numbers of cations and anions is

$$\Xi(\sigma^*) = \sum_{N=0}^{\infty}\frac{1}{(N!)^2}\exp\left(2N\ln N + N\mu/k_BT\right)\int d\underline{r}^{(2N)}\exp\left[-H_N(\sigma^*)/k_BT\right]. \tag{4.3}$$

A change in surface charge density by an amount $\Delta\sigma^*$ changes the Hamiltonian by

$$\Delta H_N = \left[-\frac{4\pi e^2}{\varepsilon d}D + \sum_{i=1}^{2N}\frac{\partial\varphi_i(z_i)}{\partial\sigma^*}\right]\Delta\sigma^* \tag{4.4}$$

and hence the partition function is changed to first order in $\Delta\sigma^*$ into

$$\Xi(\sigma^*+\Delta\sigma^*) = \Xi(\sigma^*)\left[1 + 4\pi\beta^*<D>_0\Delta\sigma^* - \beta^*<\sum_{i=1}^{2N}\frac{\partial\varphi_i(z_i)}{\partial\sigma^*}>_0\Delta\sigma^*\right], \tag{4.5}$$

where $\beta^* = e^2/(\varepsilon k_BTd)$ and $<\cdots>_0$ denotes an average on phase space weighted by $\exp\left[-H_N(\sigma^*)/k_BT\right]$. The change in the average dipole moment is then given by

$$\left[<D> - <D>_0\right]/\Delta\sigma^* = 4\pi\beta^*\left[<D^2>_0 - <D>_0^2\right]$$
$$-\beta^*\left[<D\sum_{i=1}^{2N}\frac{\partial\varphi_i(z_i)}{\partial\sigma^*}>_0 - <D>_0<\sum_{i=1}^{2N}\frac{\partial\varphi_i(z_i)}{\partial\sigma^*}>_0\right]. \tag{4.6}$$

The expression of the first term on the right-hand side of Eq.(4.6) is equivalent to a result reported earlier by Blum et al. [17] for an infinite sample. Since this expression is evaluated here on a finite sample, the second term arises in the simulation configuration from the dependence on σ^* of the interactions of the sample with the replicas. Fortunately, the potentials $\varphi_i(z_i)$ show only small fluctuations and converge rapidly to equilibrium values, thus allowing a rather reliable evaluation of $\partial\varphi_i(z_i)/\partial\sigma^*$ from the Monte Carlo density profiles. However, the two terms in Eq.(4.6) as calculated from our Monte Carlo runs show strong mutual cancellation, so that our evaluation of the differential capacitance by this method is affected by a sizable statistical uncertainty.

Our results for the capacitance $C_d(\sigma)$ of the diffuse layer in the model are reported in Fig. 8. The values obtained by using Eq.(4.6) are shown as vertical bars on account of their statistical accuracy, while the full curve shows the results obtained by numerical differentiation of the potential drop in Fig. 6. It is difficult to assess the accuracy of the latter data and we show them only over a limited range of values of σ^*, relevant to real electrolyte solutions. There still is approximate agreement, however, between the two methods at $\sigma^* \simeq 0.4$, where the figure reports only the result from Eq.(4.6).

The two independent sets of results in Fig. 8 agree in showing the appearance of structure in the capacitance curve. Such structure can be correlated with restructuring of ions in the interfactal region if one interprets C_d^{-1} as an effective thickness of the diffuse layer. Further structure is indicated at larger values of σ^* by the numerical differentiation of the potential drop data. Of course, the full inverse capacitance of the model is the sum of C_d^{-1} in Fig. 8 and of the inverse capacitance of the inner layer, the latter being determined by the distance assumed for the surface charge density from the contact distance between ions and wall.

5.   CONCLUSION

Extensive illustrations of the usefulness of various approximate theories of the restricted primitive model for the electrode/electrolyte interface at low and moderately large values of σ^* have already been given by Torrie and Valleau [4] and by Carnie and Torrie [3]. As a result of the present work we can add to their discussion with regard to the transition which occurs in the structure of the model interface on further increasing the surface charge density.

The HNC is generally accepted as a good approximation for the bulk structure of ionic liquids over a range of density and Coulomb coupling strength which goes from electrolyte solutions to molten salts. With regard to the diffuse layer, we have explicitly shown in Fig. 2 that the next term in the cluster expansion induces only rather minor changes in the interfacial density profiles up to fairly large surface charge densities corresponding to $\sigma^* = 0.25$, in the present model taken at a concentration of 1 M and a coupling strength $\beta^* \simeq 1.68$. On further increasing σ^*, however, the diffuse layer capacitance in the HNC grows rapidly towards a divergence. Preliminary calculations carried out in collaboration with Dr. J.S. Thakur indicate that such a divergence moves down towards the point of zero charge as the coupling strength and the density are increased towards values appropriate to a molten salt regime. This behaviour

should reflect the appearance and growth of oscillations in the charge density profile around any given ion in the bulk ionic liquid.

Our Monte Carlo data confirm and strengthen the conclusion of Torrie and Valleau [4] to the effect that a divergence in the diffuse layer capacitance is prevented in the "real" interface by a restructuring of the ionic density profiles. Their effect on the capacitance is clearly shown in Fig. 8. Deviations from a steadily rising capacitance curve are occurring at moderately large values of σ^*, when the first layer of counterions near the charged wall is very far from being densely packed. Thus it appears that restructuring of the interface is basically driven by the Coulomb interactions, although ionic sizes and other parameters of the model will also play a role.

From all our data and theoretical results it appears that the interfacial region is losing memory of bulk-like electrical behaviour in the range $\sigma^* \sim 0.2 \div 0.3$, at the present concentration and Coulomb coupling strength. It is theoretically satisfactory that the next term in the cluster expansion can account for restructuring of the interface at larger values of σ^*, at least at a semiquantitative level. It remains a question, of course, whether the leading 3-body corrections that we have been able to include in our theoretical calculations will suffice to handle the interface in a molten-salt regime of ionic density and temperature.

REFERENCES

1) See e.g. J. O'M. Bockris. B.E. Conway and E. Yeager (Eds.), Comprehensive Treatise of Electrochemistry (Plenum, New York, 1980).

2) Electrochemistry, Specialist Periodical Reports (Chemical Society, London).

3) S.L. Carnie and G.M. Torrie, Adv. Chem. Phys. 56, 141 (1984).

4) G.M. Torrie and J.P. Valleau, J. Chem. Phys. 73, 5807 (1980).

5) J.L. Lebowitz and J.K. Percus, J. Math. Phys. 4, 116 (1963).

6) R. Bacquet and P.J. Rossky, J. Chem. Phys. 79, 1419 (1982).

7) H. Iyetomi and S. Ichimaru, Phys. Rev. A27, 1241 (1983).

8) D. Henderson, F.F. Adraham and J.A. Barker, Molec. Phys. 31, 1291 (1976).

9) S.L. Carnie, D.Y.C. Chan, D.J. Mitchell and B.W. Ninham, J. Chem. Phys. 74, 1472 (1981).

10) J.P. Badiali, M.L. Rosinberg, D. Levesque and J.J. Weis, J. Phys. C16, 2183 (1983); A. Alastuey and D. Levesque, Molec. Phys. 47, 1349 (1982).

11) K. Ng, J. Chem. Phys. 61, 2680 (1974).

12) P. Ballone, G. Pastore and M.P. Tosi, J. Chem. Phys. 81, 3174 (1984).

13) P. Nielaba and F. Forstmann, Chem. Phys. Lett. 117, 46 (1985).

14) D. Henderson, L. Blum and J.L. Lebowitz, J. Electroanal. Chem. 102, 315 (1979).

15) J.P. Valleau and L.K. Cohen, J. Chem. Phys. 72, 5935 (1980).

16) J.P. Valleau and S.G. Whittington, in Modern Theoretical Chemistry, Vol. 5, Ed. P. Berne (Plenum, New York, 1977).

17) L. Blum, D. Henderson, J.L. Lebowitz, C. Gruber and P.A. Martin, J. Chem. Phys. 75, 5974 (1981).

Fig. 1   Leading bridge diagram for the correlations between the wall (shaded) and an ion in the fluid (circle), due to two ions (dots) over whose coordinates r_1 and r_2 integration is performed. The segments indicate wall-ion correlation functions (i.e. density profiles) and bulk ion-ion correlation functions. Sum over the species of ions 1 and 2 is also understood.

Fig. 2   Density profiles for counterions and coions next to a charge hard wall at $\sigma^* = 0.25$ versus distance z in units of the ionic diameter d. The theoretical results are shown by dashed lines (HNC) and full lines (modified HNC) while the dots give Monte Carlo results. The wall is located at $z/d = -\frac{1}{2}$.

Fig. 3   The same as Fig. 2, for $\sigma^* = 0.42$.

Fig. 4   The same as Fig. 2, for $\sigma^* = 0.70$.

Fig. 5   Bridge functions $-E_\alpha^{(4)}(z)$ for counterions (full line) and coions (dashed line) versus z/d at $\sigma^* = 0.42$.

Fig. 6   Potential drop ψ^* across the diffuse layer, in units of $k_B T/e$, versus surface charge density σ^*, in units of e/d^2. Monte Carlo results are shown by crosses for the case of oppositely charged walls and by dots for the case in which only one of the confining walls is charged. The circles report original data of Torrie and Valleau [4] for the latter configuration. The modified HNC results are shown by triangles at three values of σ^*, while the dashed curve shows the predictions of the HNC.

Fig. 7   Adsorption coefficients Γ_α of counterions (dashed line) and coions (dashed-dotted line), as excess numbers of particles per area d^2, and excess interfacial energy γ_e (full line, referred to right-hand scale), in units of $k_B T/d^2$.

Fig. 8   Monte Carlo results for the differential capacitance C_d of the diffuse layer per unit area, in units of $e^2/k_B T d^2$, versus reduced charge density σ^*.
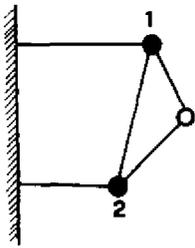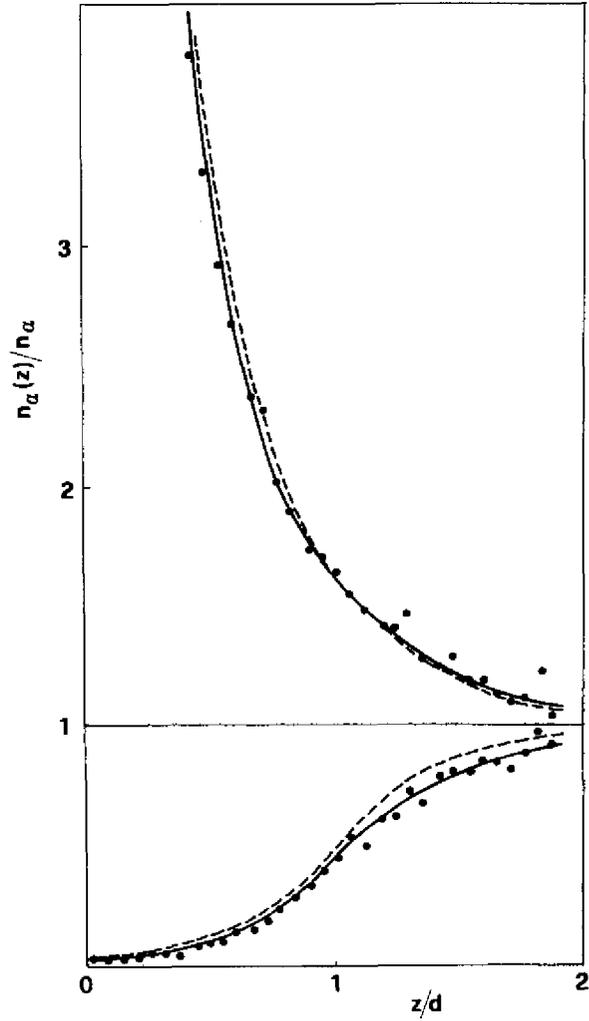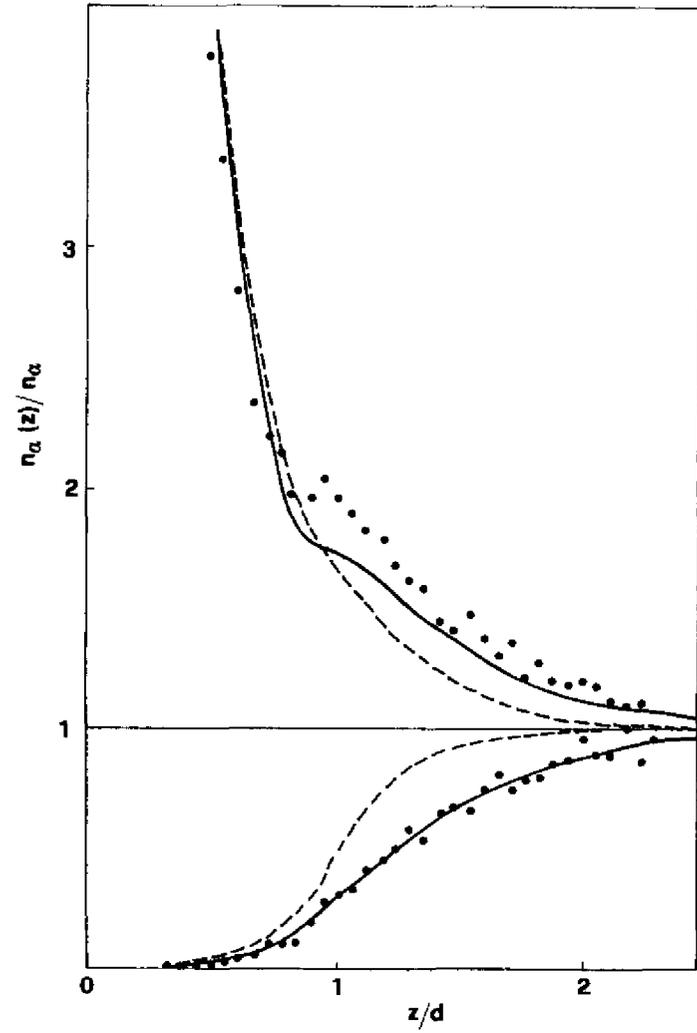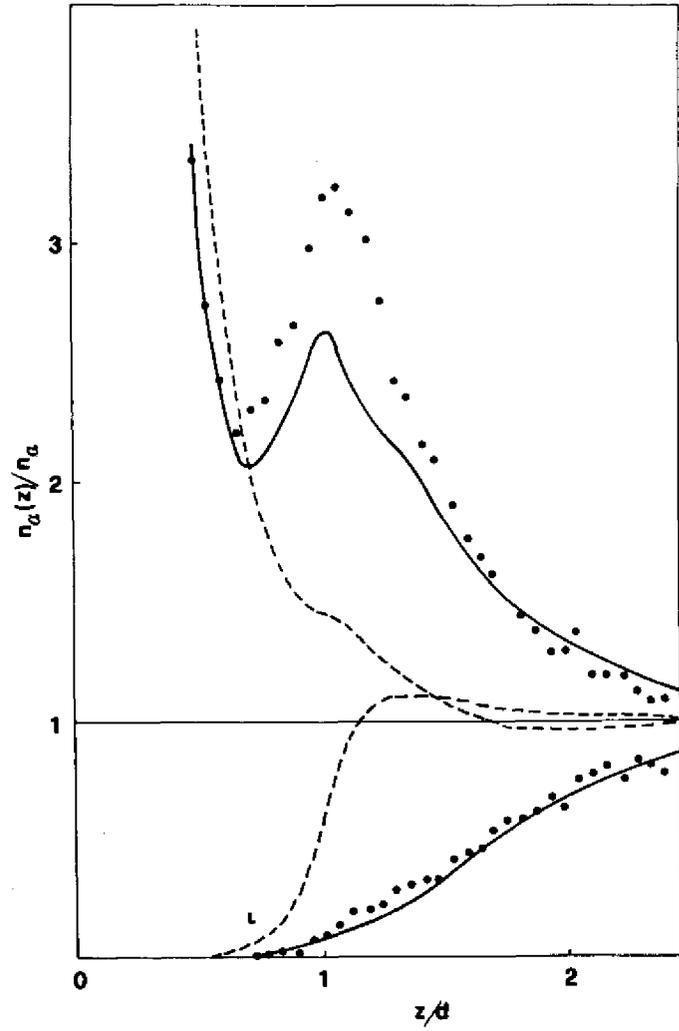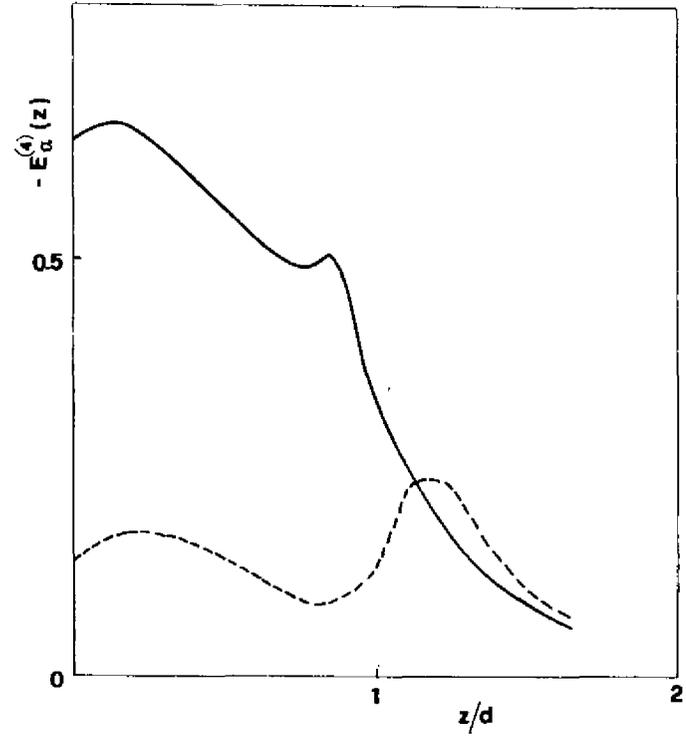
Fig.1

Fig.2

Fig.3

Fig.4

Fig.5

Fig.6

Fig.7

Fig.8